Three-Dimensional Limit Equilibrium Stability Analysis of Spile-Reinforced Shallow Tunnel

Kim, Hong-Taek*[1]
Sim, Young-Jong*[2]
Lee, Wan-Jae*[3]

요 지

Spiling reinforcement system은 매회의 터널굴진작업 이전에 막장면 주위를 따라 방사방향 및 굴진방향으로 先지반보강을 목적으로 천공을 실시하고, spile을 설치한 후 시멘트 그라우팅을 시행하여, 원지반 자체의 전단강도 증대를 통한 무지보 자립시간의 향상과 터널 주변지반의 변위 억제 및 지속적인 아칭작용 등을 유도하여 터널자체의 장기적인 안정화 및 지표면 침하억제 등을 도모하는 공법이다. 이와같은 先지반보강 개념의 spiling reinforcement system은 미국등지에서 주로 약한 암반 터널의 장기적인 안정화를 위해 사용되어져 왔으나, 최근의 연구에서는 연약한 토사지반 터널로까지 그 적용성이 점차 확대되는 경향을 보이고 있다.

본 연구의 주된 목적은, spiling reinforcement system을 적용한 약한암반 및 토사지반 터널에 대한 3차원 안정해석체계의 정립이다. 이를 위해 본 논문에서는 일차적으로, 예상파괴면의 형상이 지표면까지 확장되는 얕은 spile-reinforced 터널의 경우에 한해, 터널굴착에 따른 막장주변의 3차원적 파괴거동등을 3D FEM 해석을 통해 분석하여 종·횡방향 파괴면등 예상 파괴흙쐐기의 형상을 가정한 다음, 한계평형이론에 근거한 3차원 안정해석체계를 정립하여 터널 막장면에 대한 전체 예상안전율 평가방법을 제시하였고, 이 결과를 기존의 2차원적 해석결과와 서로 비교·분석하였다. 또한 얕은 spile-reinforced 터널과 깊은 spile-reinforced 터널을 구분하기 위한 규준의 제시가 본 연구를 통해 아울러 이루어 졌으며, 본 연구에서 제시한 이와같은 규준에 대한 적합성 확인을 위해 3D FEM 해석결과와 서로 비교가 이루어 졌다. 이외에도 제시된 규준 및 3차원 안정해석법을 토대로, 설계에 관련된 여러 변수들이 본 spiling reinforcement system이 적용된 얕은 터널에 미치는 영향등에 대해서도 분석이 이루어졌다.

Abstract

A spiling reinforcement system is composed of a series of radially installed reinforcing spiles along the perimeter of the tunnel opening ahead of excavation. The reinforcing spile network is extended into the in-situ soil mass both radially and longitudinally. The spiling

---

*1 Member, Associate professor, Department of Civil Eng., Hong-Ik University

*2 Researcher, Technology & Research, Institute Hong-Ik University

*3 Member, Senior Researcher, Construction Technology & Research Inst., LG Construction Co. LTD.

reinforcement system has been successfully used for the construction of underground openings to reinforce weak rock formations on several occasions. The application of this spiling reinforcement system is currently extended to soft ground tunneling in limited occasions because of lack of reliable analysis and design methods.

A method of three-dimensional limit equilibrium stability analysis of the spile-reinforced shallow tunnel in soft ground is presented. The shape of the potential failure wedge for the case of spile-reinforced shallow tunnel is assumed on the basis of the results of three dimensional finite element analyses. A criterion to differentiate the spile-reinforced shallow tunnel from the spile-reinforced deep tunnel is also formulated, where the tunnel depth, soil type, geometry of the tunnel and reinforcing spiles, together with soil arching effects, are considered.

To examine the suitability of the proposed method of three-dimensional stability analysis in practice, overall stability of the spile-reinforced shallow tunnel at facing is evaluated, and the predicted safety factors are compared with results from two-dimensional analyses.

Using the proposed method of three-dimensional limit equilibrium stability analysis of the spile-reinforced shallow tunnel in soft ground, a parametric study is also made to investigate the effects of various design parameters such as tunnel depth, spile length and radial spile spacing. With slight modifications the analytical method of three-dimensional stability analysis proposed may also be extended for the analysis and design of steel pipe reinforced multi-step grouting technique frequently used as a supplementary reinforcing method in soft ground tunnel construction.

Keywords : Spiling reinforcement system, 3D limit equilibrium stability analysis, Spile-reinforced shallow tunnel, 3D finite element analysis

1. Introduction

Recently, various earth reinforcement techniques have been applied to many geotechnical engineering problems. The spiling reinforcement system has been successfully used for the construction of underground openings to reinforce weak rock formations on several occasions(Korbin & Brekke, 1976, 1978). The application of this spiling reinforcement system is currently extended to soft ground tunneling in limited occasions because of lack of reliable analysis and design methods(Kim & Kwon, 1995)

A spiling reinforcement system is composed of a series of radially installed reinforcing spiles 4.5 to 6.0m long spaced between 0.5 and 1.5m with an inclination angle of approximately 30 degrees to the longitudinal tunnel axis(Bang, 1984). The reinforcing spiles are formed by inserting 2.5 to 3.8cm diameter rebars into predrilled holes with subsequent grout.

Fig. 1 shows a schematic representation of the spiling reinforcement system. The general principle deals with stabilizing a weak mass by installing an annular spiling reinforcement network along the perimeter of the tunnel opening before excavation. The purpose is to improve the stand−up time by the prevention of loosening and to contribute to permanent stabilization of the tunnel opening by the restriction of deformations. The reinforcing spile network is extended into the in−situ soil mass both radially and longitudinally.

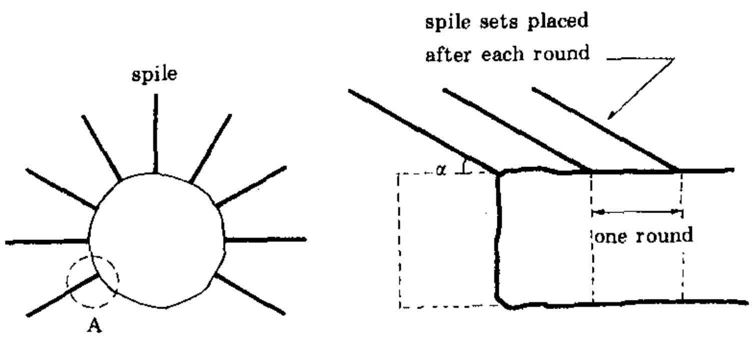

(a) Spiling reinforcement ahead of face

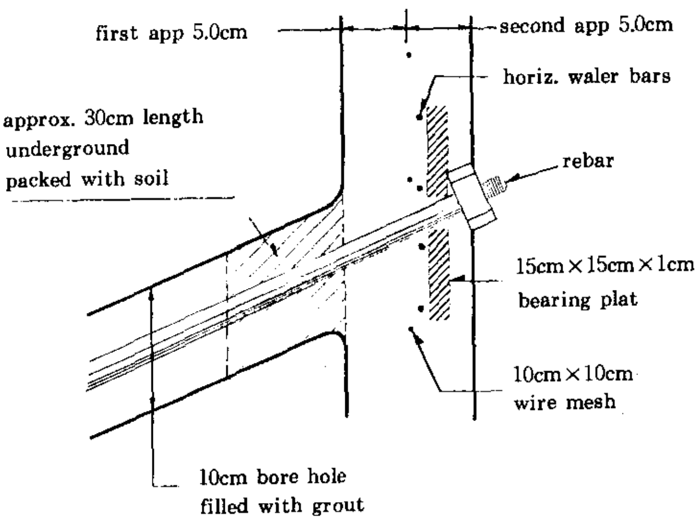

(b) Construction details(Sec. A)

Fig.1 A schematic representation of the spiling reinforcement system

A method of three-dimensional limit equilibrium stability analysis of the spile-reinforced shallow tunnel in soft ground is presented. The shape of the potential failure wedge for the case of spile-reinforced shallow tunnel is assumed on the basis of the results of three dimensional finite element analyses. A criterion to differentiate the spile-reinforced shallow tunnel from the spile-reinforced deep tunnel is also formulated considering the tunnel depth, soil type, geometry of the tunnel and reinforcing spiles, together with soil arching effects.

To examine the suitability of the proposed method of three-dimensional stability analysis in practice, overall stability of the spile-reinforced shallow tunnel at facing is evaluated, and the predicted safety factors are compared with results from two-dimensional analyses.

Using the proposed method of three-dimensional limit equilibrium stability analysis of the spile-reinforced shallow tunnel in soft ground, a parametric study is also made to investigate the effects of various design parameters such as soil type, geometry of the tunnel and reinforcing spiles.

2. Criterion for Classification of Spile-Reinforced Shallow and Deeptunnels

A criterion to differentiate the spile-reinforced shallow tunnel from the spile-reinforced deep tunnel is formulated, where the tunnel depth, soil type, geometry of the tunnel and reinforcing spiles, together with soil arching effects, are considered.

As illustrated in Fig. 2, the potential failure surface is assumed to consist of two planar surfaces bending at point A_2. The coordinates of the intersection point A_2 are $x=r+x_1 \cos\alpha_1$ and $y=x_1 \sin\alpha_1$. Also, H_c is defined as the critical depth where the maximum vertical stress σ_v is mobilized. Below the depth H_c, the vertical stress gradually decreased due to the shear resistance. Based on the critical depth H_c and tunnel depth H_1, the spile-reinforced shallow tunnel and deep tunnel are classified as follows.

If $H_c \geq H_1$, tunnel is classified as a shallow tunnel.
If $H_c < H_1$, tunnel is classified as a shallow tunnel.

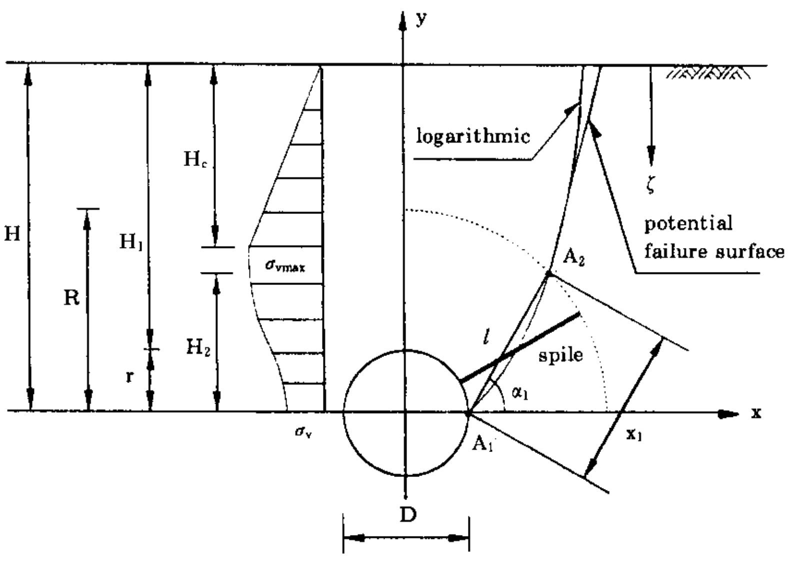

Fig.2 Potential failure surface in x－y plane

To determine the critical depth H_c, α_1 is assumed to be $45°+\phi/2$ measured from the center of the circular tunnel side. The geometric terms in Fig. 2 necessary for the formulation are as follows.

$$R=r+l\cdot\sin\theta \tag{1}$$

$$R^2=x_1^2+r^2-2x_1r\cos(\pi-\alpha_1)$$

$$x_1^2+(2r\cos\alpha_1)x_1-(R^2-r^2)=0$$

$$x_1=-r\cos\alpha_1+\sqrt{(r\cos\alpha_1)^2+(R^2-r^2)} \tag{2}$$

where, R=radius of the reinforced zone in $x-y$ plane, r= radius of the tunnel, l=length of the spile, and θ=inclination angle of the spile with z direction.

Also, $H_1=H-r$, $H_2=x_1\sin\alpha_1$, and $H_3=H-H_2$.

To solve the discontinuity problem encountered at the intersection point A_2, the potential failure surface is assumed to be a logarithmic curve which passes through the intersection points A_1 and A_2 as shown in Fig. 2. In addition,

$$(x-r)=A\cdot\ln(y+1) \tag{3}$$

where, $x=r+x_1\cos\alpha_1$ and $y=x_1\sin\alpha_1$.

Substituting these values into Eq. (3) yields

$$r+x_1\cos\alpha_1-r=A\cdot\ln(x_1\sin\alpha_1+1) \tag{4}$$

where, $A=\dfrac{x_1\cos\alpha_1}{\ln(x_1\sin\alpha_1+1)}$ Therefore, $x=\dfrac{\ln(y+1)}{\ln(x_1\sin\alpha_1+1)}(x_1\cos\alpha_1)+r$

Also, $y=H_1+r-\zeta$ and therefore,

$$x=\frac{\ln(H_1+r-\zeta+1)}{\ln(x_1\sin\alpha_1+1)}(x_1\cos\alpha_1)+r \tag{5}$$

In addition, $B=2x$ and the following expression is finally obtained.

$$\begin{aligned}\frac{d\sigma_v}{d\zeta}&=\gamma-\frac{2c}{B}-2K_a\gamma\zeta\frac{\tan\phi}{B}\\&=\gamma-\frac{c\cdot\ln(x_1\sin\alpha_1+1)}{\ln(H_1+r-\zeta+1)(x_1\cos\alpha_1)+r\cdot\ln(x_1\sin\alpha_1+1)}\\&\quad-K_a\gamma\zeta\tan\phi\frac{\ln(x_1\sin\alpha_1+1)}{\ln(H_1+r-\zeta+1)(x_1\cos\alpha_1)+r\cdot\ln(x_1\sin\alpha_1+1)}\end{aligned} \tag{6}$$

By differentiating Eq. (6) with respect to depth ζ and equating the result to zero, i.e., $\dfrac{d\sigma_v}{d\zeta}=0$, the maximum vertical stress σ_v and the critical depth H_c are determined. Below this critical depth H_c, soil arching effects are expected to occur.

Compared with the results from 3D FEM analyses by Kim et al.(1996), the proposed criterion described above shows generally good agreement. The results of the comparisons are summarized in Table 1. Based on Table 1, a schematic criterion of the classification of the spile-reinforced shallow and deep tunnels for various depths and different soil internal friction angles can be also drawn as Fig. 3. For example, if $\phi=42°$ and $H_1/D=1$, the corresponding tunnel is classified as a shallow tunnel. However, if $\phi=42°$ and $H_1/D=3$, the corresponding tunnel is classified as a deep tunnel. And although the case of $\phi<22°$ is not shown in Fig. 3, the corresponding tunnel is classified as a shallow tunnel within a given range.

Table 1. Comparisons with 3D FEM analyses results carried out by Kim et al.(1996)

soil internal friction angle ϕ(°)	Results of classification based on the proposed criterion						3D FEM analyses		
	$H_1/D=1$		$H_1/D=3$		$H_1/D=5$		$\frac{H_1}{D}=1$	$\frac{H_1}{D}=3$	$\frac{H_1}{D}=5$
	H_c(m)	result	H_c	result	H_c	result			
22	–	Shallow	–	Shallow	–	Shallow	–	Shallow	Shallow
32	–	Shallow	15.55	Deep	18.51	Deep	Shallow	Deep	Deep
42	–	Shallow	10.64	Deep	11.70	Deep	Shallow	Deep	Deep
52	–	Shallow	6.58	Deep	6.90	Deep	Shallow	Deep	Deep
62	3.54	Deep	3.60	Deep	3.62	Deep	Deep	Deep	–

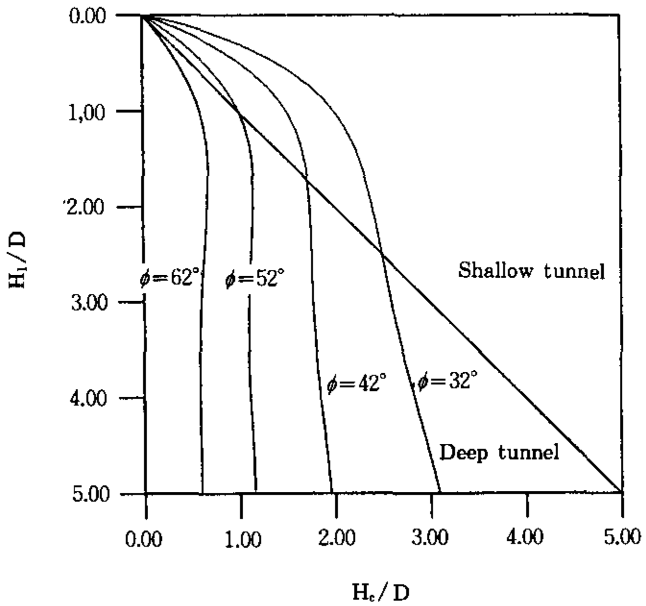

Fig.3 A schematic criterion of classification of the spile-reinforced shallow and deep tunnel

3. 3D FEM Analysis

To determine the postulated three dimensional failure wedge which lies ahead of the spile-reinforced tunnel facing, 3D FEM analyses are carried out for the case of a shallow tunnel. The 'SMAP 3D' Program is used for 3D FEM analyses. In these 3D FEM analyses, soil and shotcrete are modeled as continuum elements and the spile is considered as a truss element which only mobilizes frictional resistance due to the small diameter of the spile itself. Although tensile forces constitute the dominant reinforcing mechanism, passive lateral earth resistance can develop against the spile on either side of a potential failure surface, when reinforcing elements are rigid. Pertinent parameters and grid model used in 3D FEM analyses are summarized in Table 2 and Fig. 4.

Table 2. Pertinent parameters used in 3D FEM analyses

soil unit weight $\gamma(t/m^3)$	soil cohesion $c(t/m^2)$	soil internal friction angle $\phi(°)$	tunnel diameter D(m)	tunnel depth H(m) (refer to Fig.2)	spile length ℓ (m)	inserting angle of spile(°)	longitudinal spile spacing s_l(m)	radial spile spacing s_r(m)
1.8	1.5	30	6.0	12.0	6.0	30	1.3	0.5

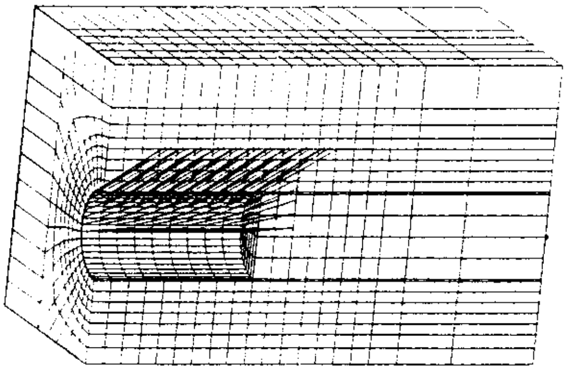

Fig.4 Grid model used in 3D FEM analyses

A typical shear strain distribution obtained by 3D FEM analyses is depicted by the contours in Fig. 5. The postulated three dimensional failure wedge is approximately estimated by examining the locus of the points of maximum shear strain.

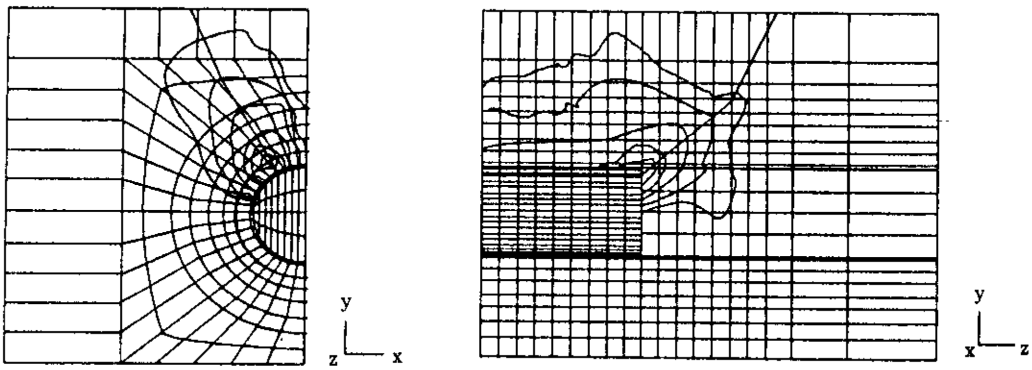

(a) Shear strain distribution in transverse direction

(b) Shear strain distribution in longitudinal direction

Fig.5 Results of 3D FEM analyses

4. Three Dimensional Limit Equilibrium Stability Analysis of the Spile-Reinforced Shallow Tunnel

4.1 Assumptions

Postulated shape of the three dimensional failure wedge is approximated by connecting the highest maximum shear strain points on x−y plane and y-z plane analyzed through 3D FEM analyses. It appears that the shape of the postulated three dimensional failure wedge for the case of the spile-reinforced shallow tunnel may be reasonably assumed to consist of two planar surfaces with a transition occurring at the back edge of the spile-reinforced zone as shown in Fig. 6.

In addition, the postulated three dimensional failure wedge in Fig. 6 has angles α_1 and α_3 in the spile−reinforced soil region, and angles α_2, α_4 and α_5 in the unreinforced soil region starting from the side of the tunnel with the same elevation as the center line of the tunnel. Note that the conditions $\alpha_2 \geq \alpha_1$ and $\alpha_4 \geq \alpha_3$ are required when performing the analysis. Note also that angles α_2 and α_4 are the same because the soil deposits are assumed to be homogeneous. An angle α_3 is assumed to have an angle of $\tan^{-1}(H_2/l\cos\theta)$ as shown in Fig. 6. The three dimensional failure wedge is determined by finding a set of angles which yields the lowest overall factor of safety.

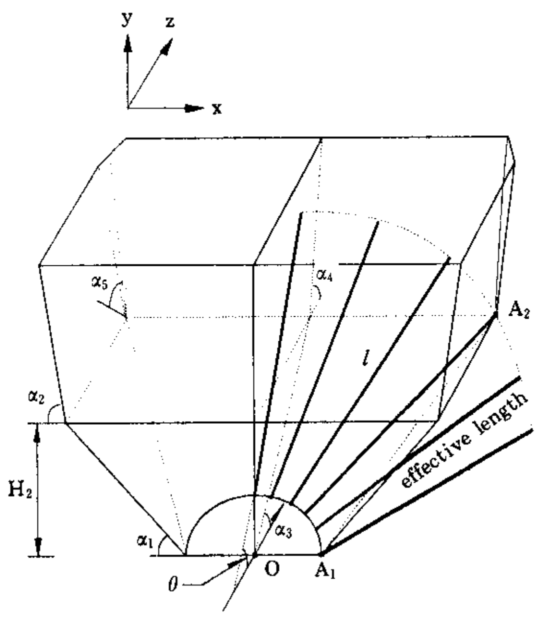

Fig.6 Postulated shape of the three dimensional failure wedge

Because of the symmetry of a tunnel axis and planes of failure about the y−z plane, only half of the failure wedge needs to be considered. Note that no shearing forces are expected in the plane of symmetry.

It is further assumed that the direction of the failure wedge movement is within the y−z plane only, and therefore the horizontal shear stresses are assumed to be zero on the x−y plane. The shear forces acting on the y-z plane are assumed to be parallel to the bottom surface of the failure wedge. For example, the shear force S_2 and the projection of the S_4 and S_6 on y−z plane have an angle α_3 with z axis. This assumption is similar to the assumption adopted in the three dimensional slope stability analysis described by Chen and Chameau(1982). Taking into account the assumptions described above, the free body diagram of the three dimensional failure wedge may be drawn as shown in Fig. 7.

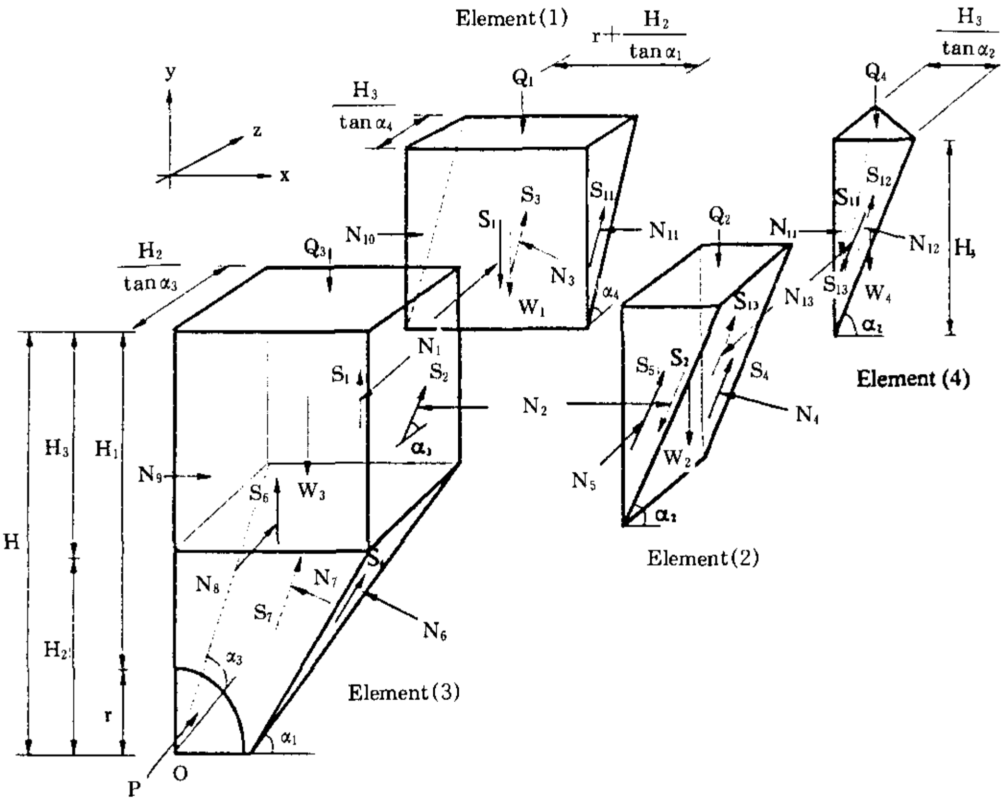

Fig.7 Resulting free body diagram of the three dimensional failure wedge

4.2 Formulations

As shown in Fig. 8, the forces acting on the Element(4) are determined as follows.

$$W_4=\frac{\gamma}{6}\cdot\frac{H_3^3}{\tan\alpha_2\tan\alpha_4} \tag{7}$$

$$Q_4=\frac{q}{2}\cdot\frac{H_3^2}{\tan\alpha_2\tan\alpha_4} \tag{8}$$

$$N_{11}=\frac{1}{6}K_0\gamma\frac{H_3^3}{\tan\alpha_4}=N_{10}, \quad S_{11}=\beta_{11}N_{11} \tag{9}$$

$$N_{13}=\frac{1}{6}K_0\gamma\frac{H_3^3}{\tan\alpha_2}=N_5, \quad S_{13}=\beta_{13}N_{13} \tag{10}$$

where, W_4=weight of Element(4), q=surcharge per unit area of ground surface, Q_4=total force caused by surcharge q, γ=unit weight of soil, K_o=coefficient of earth pressure at rest, and β_{11}, β_{13}=ratios between normal and tangential forces.

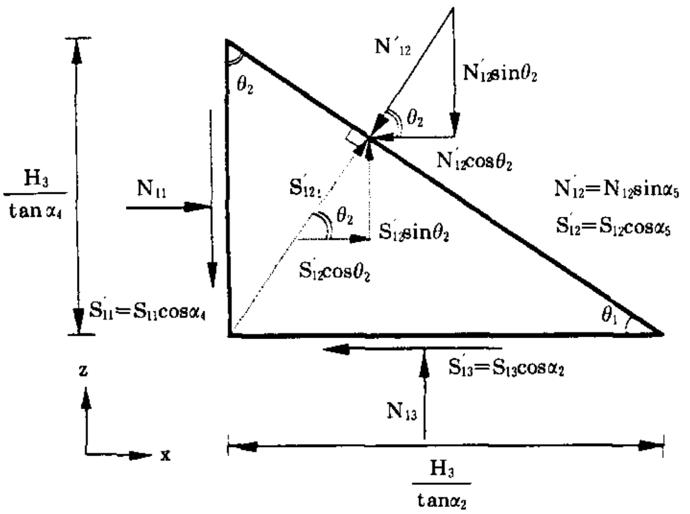

Fig.8 Forces acting on Element(4) in x−z plane

Based on the force equilibrium conditions, normal and tangential forces could be estimated. To estimate the ratio β, it is assumed that the total driving force expected along the postulated failure surfaces is equal to the total resisting force developed along the same failure surfaces, i.e.,

$$N_{12}=(W_4+Q_4+S_{11}\sin\alpha_4+S_{13}\sin\alpha_2)\cos\alpha_5+(N_{11}-S_{13}\cos\alpha_2)\frac{\sin\alpha_5}{\cos\theta_2}$$

$$S_{12}=(W_4+Q_4+S_{11}\sin\alpha_4+S_{13}\sin\alpha_2)\sin\alpha_5+(N_{11}-S_{13}\sin\alpha_2)\frac{\cos\alpha_5}{\cos\theta_2} \tag{11}$$

$$=N_{12}\tan\phi'+\frac{c'}{2}\cdot\frac{H_3}{\tan\alpha_2}\cdot\frac{H_3}{\tan\alpha_4}\cdot\sec\alpha_5$$

$$N_{12}=(W_4+Q_4+S_{11}\sin\alpha_4+S_{13}\sin\alpha_2)\cos\alpha_5+(N_{13}-S_{11}\cos\alpha_4)\frac{\sin\alpha_5}{\sin\theta_2}$$

$$S_{12}=(W_4+Q_4+S_{11}\sin\alpha_4+S_{13}\sin\alpha_2)\sin\alpha_5+(N_{13}-S_{11}\cos\alpha_2)\frac{\cos\alpha_5}{\sin\theta_2} \tag{12}$$

$$=N_{12}\tan\phi'+\frac{c'}{2}\cdot\frac{H_3}{\tan\alpha_2}\cdot\frac{H_3}{\tan\alpha_4}\cdot\sec\alpha_5$$

where, c'=developed soil cohestion, ϕ'=developed soil internal friction angle, α_5=angle between the plane acting on the shear force S_{12} and the horizontal plane.

By solving Eqs. (9)~(12), the ratios between the normal and tangential forces, β_{11} and β_{13}, are determined as follows.

$$\beta_{11}=\frac{BF+DC}{AD-BE},\ \beta_{13}=\frac{CE+AF}{AD-BE} \tag{13}$$

where, $A=N_{11}\sin\alpha_4(\sin\alpha_5-\cos\alpha_5\tan\phi')$

$$B=N_{13}\sin\alpha_2(\cos\alpha_5\tan\phi'-\sin\alpha_5)-N_{13}\cos\alpha_2(\frac{\mathrm{som}\alpha_5}{\cos\theta_2}\tan\phi'+\frac{\cos\alpha_5}{\cos\theta_2})$$

$$C=(W_4+Q_4)(\cos\alpha_5\tan\phi'-\sin\alpha_5)+N_{11}(\frac{\sin\alpha_5}{\cos\theta_2}\tan\phi'+\frac{\cos\alpha_5}{\cos\theta_2})+\frac{c'H_3^2}{2\tan\alpha_2\tan\alpha_4\cos\alpha_5}$$

$$D=N_{13}\sin\alpha_2(\sin\alpha_5-\cos\alpha_5\tan\phi')$$

$$E=N_{11}\sin\alpha_4(\cos\alpha_5\tan\phi'-\sin\alpha_5)-N_{11}\cos\alpha_4(\frac{\sin\alpha_5}{\sin\theta_2}\tan\phi'+\frac{\cos\alpha_5}{\sin\theta_2})$$

$$F=(W_4+Q_4)(\cos\alpha_5\tan\phi'-\sin\alpha_5)+N_{13}(\frac{\sin\alpha_5}{\sin\theta_2}\tan\phi'+\frac{\cos\alpha_5}{\sin\theta_2})+\frac{c'H_3^2}{2\tan\alpha_2\tan\alpha_4\cos\alpha_5}$$

Since the tangential force cannot be greater than the maximum shear resistance $N\tan\phi'$, the ratio β must be smaller than $\tan\phi'$. Value of the ratio β, therefore, must be positive, i.e.,

$$0.0\le\beta\le\tan\phi'$$

Also the forces acting on Element(2) are determined as follows.

$$W_2=\frac{\gamma}{2}\cdot\frac{H_3^2}{\tan\alpha_2}\cdot\frac{H_2}{\tan\alpha_3} \tag{14}$$

$$Q_2=q\cdot\frac{H_3}{\tan\alpha_2}\cdot\frac{H_2}{\tan\alpha_3} \tag{15}$$

$$N_5=\frac{1}{6}\cdot K_0\cdot\gamma\cdot\frac{H_3^3}{\tan\alpha_2},\quad S_5=N_5\cdot\tan\phi'+\frac{c'}{2}\cdot\frac{H_3^2}{\tan\alpha_2} \tag{16}$$

$$N_2=\frac{1}{2}K_a\cdot\gamma\cdot H_3^2\cdot\frac{H_2}{\tan\alpha_3},\quad S_2=\beta_2N_2 \tag{17}$$

where W_2=weight of Element(2), Q_2=total force caused by *surcharge* q.

Based on the force equilibrium conditions of Element(2), normal force N_4 and tangential force $S'_4(=S_4\sin\alpha_3)$ are determined as follows.

$$\begin{aligned}N_4&=(W_2+Q_2+S_2\sin\alpha_3)\cos\alpha_2+N_2\sin\alpha_2\\ S'_4&=(W_2+Q_2+S_2\sin\alpha_3)\sin\alpha_2-N_2\cos\alpha_2-S_{13}-S_{15}\\ &=(N_4\tan\phi'+c'\cdot\frac{H_2}{\tan\alpha_3}\cdot\frac{H_3}{\sin\alpha_2})\cdot\sin\alpha_3\end{aligned} \tag{18}$$

From the above equations, ratio $\beta_2 (0.0 \le \beta_2 \le \tan\phi')$ is estimated as follow.

$$\beta_2 = [(W_2 + Q_2 \sin\alpha_2 - N_2 \cos\alpha_2 - S_{13} - S_5 - \{(W_2 + Q_2)\cos\alpha_2 + N_2 \sin\alpha_2\}\tan\phi' \sin\alpha_3 - \frac{c' H_2 H_3 \sin\alpha_3}{\tan\alpha_3 \sin\alpha_2}]$$

$$\div N_2 \sin\alpha_3 (\cos\alpha_2 \sin\alpha_3 \tan\phi' - \sin\alpha_2) \tag{19}$$

Also the forces acting on Element(1) are determined as follows.

$$W_1 = \frac{1}{2} \cdot \gamma \cdot \frac{H_3^2}{\tan\alpha_4}(r + \frac{H_2}{\tan\alpha_1}) \tag{20}$$

$$Q_1 = q \cdot (r + \frac{H_2}{\tan\alpha_1})\frac{H_3}{\tan\alpha_4} \tag{21}$$

$$N_1 = \frac{1}{2} K_a \gamma H_3^2 (r + \frac{H_2}{\tan\alpha_1}), \quad S_1 = \beta_1 N_1 \tag{22}$$

where W_1=weight of Element(1), Q_1=total force caused by surcharge q.

Based on the force equilibrium conditions of Element(1), normal and tangential forces are determined as follows.

$$\begin{aligned} N_3 &= (W_1 + Q_1 + S_1)\cos\alpha_4 + N_1 \sin\alpha_4 \\ S_3 &= (W_1 + Q_1 + S_1)\sin\alpha_4 - N_1 \cos\alpha_4 - S_{11} \\ &= N_3 \tan\phi' + c' \frac{H_3}{\sin\alpha_4}(r + \frac{H_2}{\tan\alpha_1}) \end{aligned} \tag{23}$$

From the above equations, ratio $\beta_1 (0.0 \le \beta_1 \le \tan\phi')$is estimated as follows.

$$\beta_1 = [(W_1 + Q_1)\sin\alpha_4 - N_1 \cos\alpha_4 - S_{11} - \{(W_1 + Q_1)\cos\alpha_4 + N_1 \sin\alpha_4\}\tan\phi'$$

$$- c' \frac{H_3}{\sin\alpha_4}(r + \frac{H_2}{\tan\alpha_1})] \div N_1 (\cos\alpha_4 \tan\phi' - \sin\alpha_4) \tag{24}$$

As shown in Fig.7, the forces acting on Element(3) are determined as follows.

$$W_3 = \gamma \cdot \{\frac{H_2 H_3}{\tan\alpha_3}(r + \frac{H_2}{\tan\alpha_1}) + \frac{1}{6}\frac{H_2^2}{\tan\alpha_3}(3r + \frac{2H_2}{\tan\alpha_1})\} \tag{25}$$

$$Q_3 = q \cdot \frac{H_2}{\tan\alpha_3}(r + \frac{H_2}{\tan\alpha_1}) \tag{26}$$

$$\begin{aligned} N_8 &= \frac{1}{2} K_a \gamma H^2 (r + \frac{H_2}{\tan\alpha_1}) - \frac{1}{6}\frac{H_2^2}{\tan\alpha_1}(2K_a \gamma H_2 + 3K_a \gamma H_3) - \frac{1}{4}\pi r^2 K_a \gamma H + \frac{1}{8}\pi r^3 K_a \gamma \\ S_8 &= N_8 \tan\phi' + c' \{H_3 (r + \frac{H_2}{\tan\alpha_1}) + (2r + \frac{H_2}{\tan\alpha_1})\frac{H_2}{2} - \frac{\pi r^2}{4}\} \end{aligned} \tag{27}$$

where W_3=weight of Element(3), Q_3=total force caused by surcharge q.

As previously defined, no shearing forces are expected on the plane of symmetry. As a result, the normal force N_9 acting on this plane may be reasonably assumed to be an at-rest condition, i.e.,

$$N_9 = \frac{1}{2} K_0 \gamma \frac{H_2 H_3^2}{\tan\alpha_3} + \frac{1}{2} K_0 \gamma \frac{H_2^2 H_3}{\tan\alpha_3} + \frac{1}{6} K_0 \gamma \frac{H_2^3}{\tan\alpha_3} \tag{28}$$

In addition, the force equilibrium conditions in all directions for the spile-reinforced soil block Element(3) yields the following.

$$N_6\cos\alpha_1+S_6\sin\alpha_1\sin\alpha_3+N_7\cos\alpha_3+S_7\sin\alpha_3=Q_3+W_3+S_8-S_1-S_2\sin\alpha_3$$
$$N_6\sin\alpha_1-S_6\cos\alpha_1\sin\alpha_3=N_9-N_2 \tag{29}$$

$$S_6\sin\alpha_1\cos\alpha_3-N_7\sin\alpha_3+S_7\cos\alpha_3=N_1-N_8-P-S_2\cos\alpha_3$$

where, P=total force caused by compressed air.

Furthermore considering the overall moment equilibrium condition about point O, and using the above Eq. (29), the following equation is obtained.

$$N_6\cdot h_{N6}-S_6\sin\alpha_1\cdot h_{S6}+N_7\cdot h_{N7}$$
$$=P\cdot h_p+Q_3\cdot h_{Q3}+W_3\cdot h_{W3}+N_8\cdot h_{N8}+S_2\cdot h_{S2}-S_1\cdot h_{S1}-N_1\cdot h_{N1} \tag{30}$$

where h_P, h_{Q3}, h_{N8}, h_{W3}, h_{S2}, h_{S1}, h_{N1}, h_{N6}, h_{S6}, and h_{N7}, are the moment arms of the related acting forces to the reference point O. By solving the above equations, forces N_6, S_6, N_7 and S_7 are determined.

The total driving force expected along the entire postulated failure surfaces is as follows.

$$S_D=S_3+S_4+S_5+S_6+S_7+S_8+S_{12} \tag{31}$$

The total resisting force developed along the entire postulated failure surfaces may be determined as follows.

$$S_F=(N_3+N_4+N'_6+N_7+N_8+N_{12})\cdot\tan\phi'$$
$$+c'\cdot\{\frac{H_3}{\sin\alpha_4}(r+\frac{H_2}{\tan\alpha_1})+\frac{H_2}{\tan\alpha_3}\frac{H_3}{\sin\alpha_2}+\frac{H_2}{2\tan\alpha_3}\frac{H_2}{\sin\alpha_1}$$
$$+\frac{H_2}{2\sin\alpha_3}(2r+\frac{H_2}{\tan\alpha_1})+\frac{H_3^2}{2\tan\alpha_2\tan\alpha_4\cos\alpha_5}+H_3(r+\frac{H_2}{\tan\alpha_1})$$
$$+(2r+\frac{H_2}{\tan\alpha_1})\frac{H_2}{2}+\frac{1}{2}\frac{H_3^2}{\tan\alpha_2}-\frac{\pi r^2}{4}\}+\Sigma T_{TT} \tag{32}$$

where, $N'_6=N_6+\Sigma T_{TN}$, $T_{TN}=T_T\sin(\alpha_1+\theta_n-90°)$

$T_{TT}=T_T\cos(\alpha_1+\theta_n-90°)$, $T_T=T_n\sin\theta$,

θ_n=angle between the projection of the spile on x−y plane and y axis

θ=inclination angle between the spile and z direction

The maximum spile tension expressed as T_n in Eq. (32) is expected to occur at the intersection point between the postulated failure surface and the corresponding spile. Value of T_n is estimated by integrating the shear stresses developed between the reinforcing spile and the surrounding soil, based on the mean value over the effective spile length of the normal stresses in the transformed axis which is in the plane perpendicular to the spile, i.e.,

$$T_n=\frac{\pi d_{spile}l_n(\sigma_m\tan\phi'+c')}{s_l}\le(A_{spile}\ f_y/s_l) \tag{33}$$

where, d_{spile}=spile diameter, s_l=longitudinal spile spacing, A_{spile}=cross-sectional area of reinforcing spile, l_n=effective length of nth spile, f_y=tensile yield strength of spile, σ_m =mean value of the normal stresses.

The effective length is dependant on the point of intersection between the reinforcing spiles and the assumed failure surface. When a reinforcing spile intersects the assumed failure surface at point c as shown in Fig. 9, the effective length can be calculated through following procedures.

$$cb = R_n \cos\theta_n = x_n \sin\alpha_1 \tag{34}$$

where, $\nu \le \theta_n \le \frac{\pi}{2}$, $\nu = \cos^{-1}\frac{H_2}{R}$ (refer to Fig.2)

$$R_n^2 = x_n^2 + r^2 2x_n r \cos\alpha_1 \tag{35}$$

From Eq. (34) and (35)

$$R_n = \{\frac{-B + \sqrt{B^2 - 4A}}{2A}\} \cdot r \tag{36}$$

where, $A = (\frac{\cos\theta_n}{\sin\alpha_1}) - 1$ and $B = 2(\frac{\cos\theta_n}{\tan\alpha_1})$

therefore, the effective length l_n can be calculated as Eq. (37).

$$l_n = l - \frac{R_n - r}{\sin\theta} \tag{37}$$

where, l=total length of the spile, θ=inclination of the spile

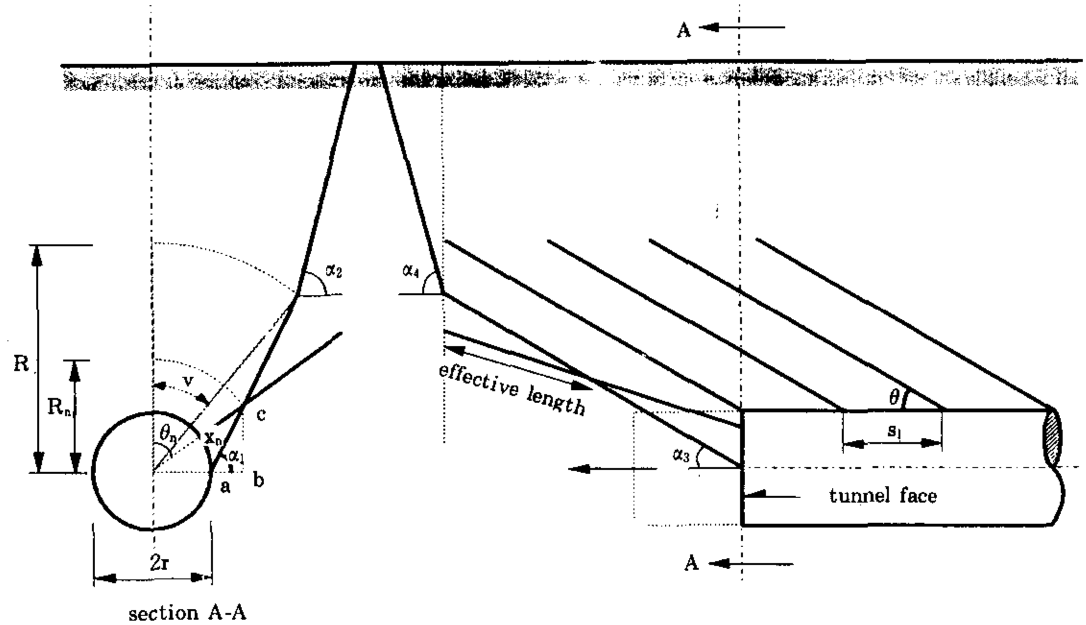

Fig.9 Parameters goveming force on spile

4.3 Evaluation of overall stability

Based on the equilibrium conditions, the three dimensional overall stability of the spile-reinforced shallow tunnel system may be analyzed. At any stage of analysis, the total driving force and the total developed resisting force along the postulated three dimensional failure wedge surfaces must be in equilibrium state, i.e.,

$$S_D = S_F \tag{38}$$

The overall factor of safety of this system, FS, is estimated on the basis of the Taylor's criterion.

$$FS_c = FS_\phi = FS \tag{39}$$

where FS_c=factor of safety with respect to soil cohesion and FS_ϕ=factor of safety with respect to soil internal friction angle.

The factor of safety with respect to cohesion and friction is regarded as the ratio between the available cohesion and friction and the developed cohesion and friction, i.e.,

$$c' = c / FS, \ \tan'\phi = \tan\phi / FS \tag{40}$$

By solving the derived equilibrium equations, the overall three-dimensional factor of safety of the spile-reinforced shallow tunnel system, FS, may finally be determined. An iterative solution procedure for determination of FS is necessary for various angles defining shapes of the postulated failure wedge.

5. Comparison with the Mostafa's Two Dimensional Analysis

In 1982 Mostafa presented a two-dimensional stability analysis method for the spiling reinforcement system. The overall factors of safety predicted by the proposed method of analysis on the basis of the postulated three dimensional failure wedges of the spile-reinforced shallow tunnels are compared with the results from the two dimensional stability analysis method by Mostafa. Table 3 describes values of pertinent parameters used for the analysis. Also the predicted results of factors of safety are described and compared in Fig. 10.

Table 3. Values of pertinent parameters used in the analyses

soil unit weight $\gamma(t/m^3)$	soil cohesion $c(t/m^2)$	soil internal friction angle $\phi(°)$	tunnel diameter D(m)	tunnel depth H(m) (refer to Fig.7)	spile length ℓ (m)	inserting angle of spile(°)	spile spacing $s_l = s_r$(m)
1.9	1.95	33	6.1	9.14 12.2	0.75D	30	0.3~0.9

As illustrated in Fig. 10, in the case of tunnel depth H=9.14m, three dimensional factors of safety are predicted as 11~20% higher than those of two dimensional factors of safety. In the case of tunnel depth H=12.2m, however, two dimensional factors of safety are estimated as 11~22% higher than those of three dimensional factors of safety. The reason for this phenomenon is partly attributed to the increase in rate of total driving force expected as the tunnel depth increases because the weight increase of failure wedge is higher than that of total resisting force acting on the failure wedge surfaces.

Although the results of comparison shown in Fig. 10 are limited occasions, the overall stability of the spile-reinforced shallow tunnel at facing may be checked deliberately as the tunnel depth increases.

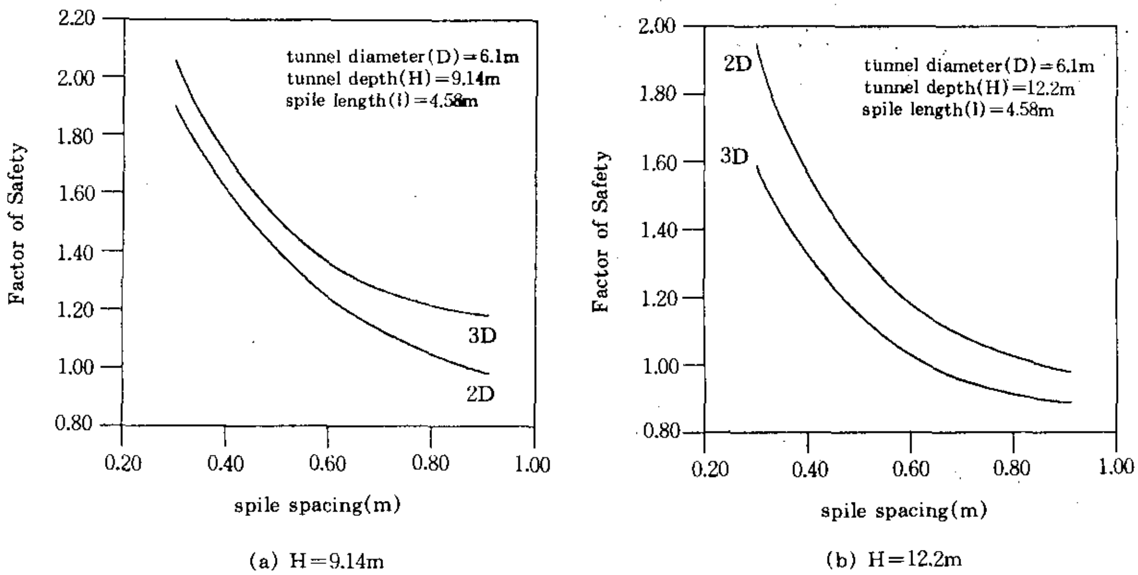

Fig.10 Results of Comparison with two dimensional analysis

6. Parametric Study

Using the proposed method of three-dimensional limit equilibrium stability analysis of the spiling reinforcement system, an analytical parametric study is carried out to investigate the effects and significances of various pertinent parameters for the spile-reinforced shallow tunnels. Properties of soil used in this parametric study are described in Table 4. The parameters selected are the tunnel depth, spile length and radial spile spacing. The adopted values for these parameters are summarized in Table 5.

Table 4. Properties of soil used in the parametric study

soil unit weight $\gamma(t/m^3)$	soil internal friction angle $\phi(°)$	soil cohesion $c(t/m^2)$
1.8	30	1.5

Table 5. Values of pertinent parameters used in the parametric study

tunnel dia. D(m)	tunnel depth H(m)	rebar dia. (cm)	spile dia. (cm)	spile length ℓ (m)	inserting angle of spile $\theta(°)$	tensile yield strength of spile (t/m^2)	longitudinal spile spacing $s_l(m)$	radial spile spacing $s_r(m)$
6	D~2D	2.5	10	0.8D~1.3D	30	35000	0.6~1.6	0.3~1.3

6.1 Effect of the tunnel depth

The tunnel depth is one of the most important parameters governing the deformation characteristics of the spile reinforcement system. For the case of shallow tunnels the factors of safety decrease as the tunnel depth increases as shown in Fig. 11. However, the decreasing rate is gradually reduced. The results in Fig. 11 show that if longitudinal spile spacing(s_l) is 1.0m, decreasing percentage rate of the factor of safety is about 28% as the tunnel depth ratio(H/D) increases from H/D=4/3 to H/D=5/3, and also the decreasing percentage rate of the factor of safety is about 20% as the tunnel depth ratio (H/D) increases from 5/3 to 6/3. These results indicate that the effects of the developed soil resistances expected along the failure wedge surfaces are relatively higher as the tunnel depth increases.

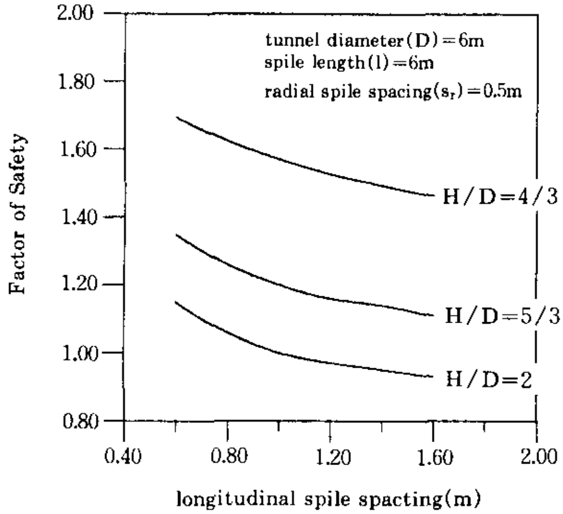

Fig.11 Effect of the tunnel depth

6.2 Effect of the spile length

The spile length is one of the most important factors in the stability of the spile reinforced tunnels in soft grounds. The effect of the spile length is analyzed with various design parameters. Fig. 12 shows that for a given tunnel depth, the factors of safety increase in general with increasing spile length.

Fig. 13 also shows the relationship between the depth ratio and the spile length for given spile spacing. According to the results shown in Fig. 13, the overall factors of safety decrease to about 59~67% for given spile length as the depth ratio increases. The results in Fig. 12 indicate that the overall factors of safety decrease to about 15~24% for given tunnel depth as the spile spacing increases. When the two results with decreasing rates of factors of safety are compared for the case of shallow tunnels, the effect of tunnel depth is more important than the effect of spile spacing.

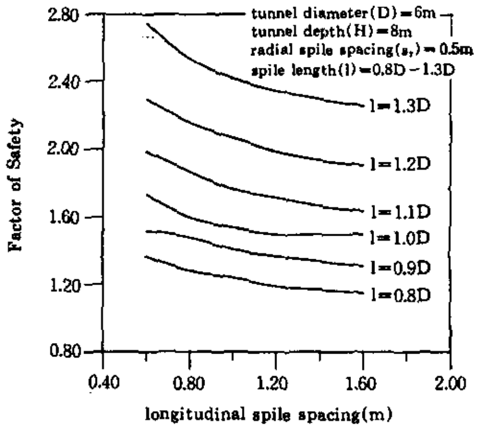

(a) H=8m

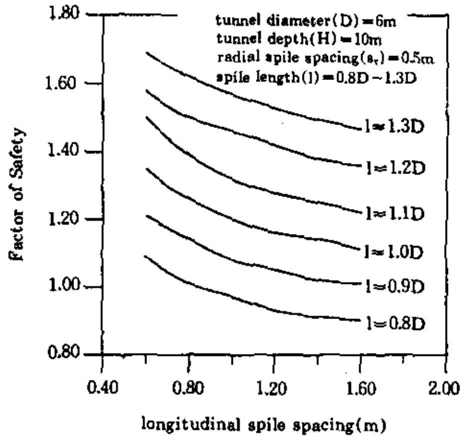

(b) H=10m

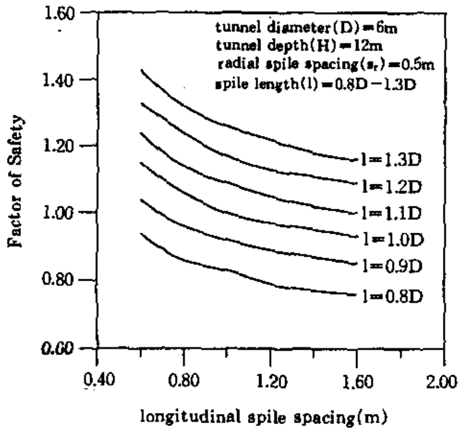

(c) H=12m

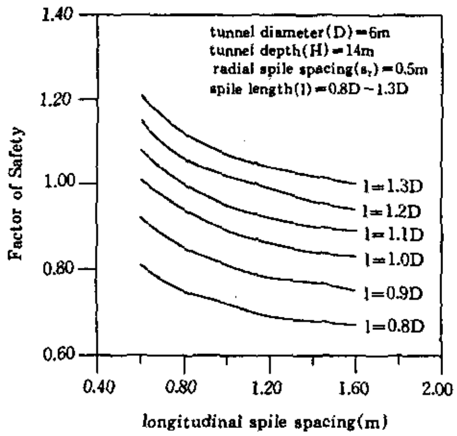

(d) H=14m

Fig.12 Effect of the spile length

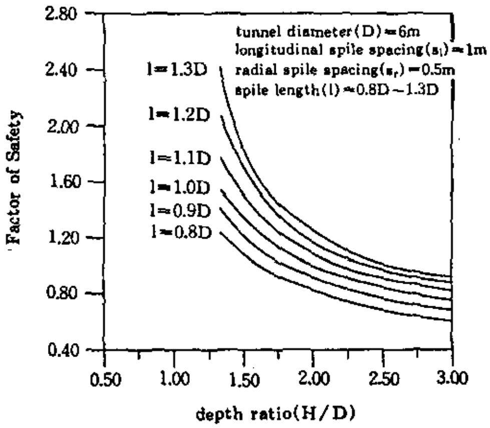

Fig.13 Relationship between the depth ratio and spile length

6.3 Effect of the radial spile spacing

The radial spacing of spile is one of the most important factors in the stability of the tunnel facing. As shown in Fig. 14, the overall factors of safety increase as the radial spacing for given spile length decreases. For example, if the radial spacing of spile is 1.3m, the decreasing percentage rate of factors of safety is about 11%. The radial spacing is 0.3m, the decreasing percentage rate of factors of safety is about 28%. These results indicate that the radial spacing of spile considerably affects the stability of the tunnel facing.

On the other hand, as the radial spile spacing increases for given spile length, the overall factors of safety gradually decrease until the improvement due to the spile reinforcement becomes negligible.

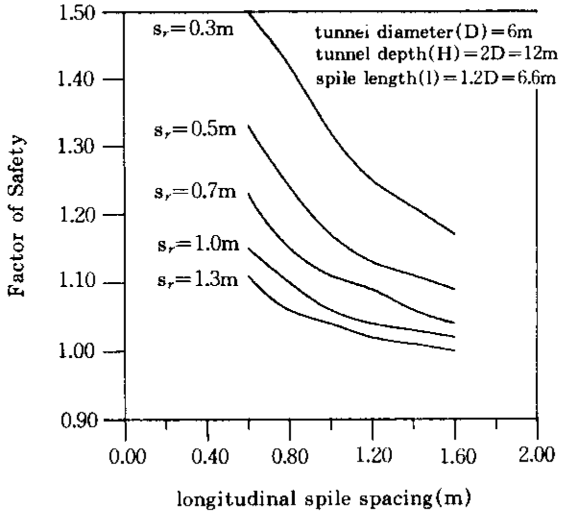

Fig.14 Effect of the radial spile spacing

7. Conclusions

A three dimensional analytical method is proposed for evaluating the stability of the spile-reinforced shallow tunnel system. A limit equilibrium analysis is performed to predict the overall factor of safety and establish a design method for the system.

A shape of the potential failure wedge for the case of spile-reinforced shallow tunnel is assumed on the basis of the results of three dimensional finite element analyses. A criterion to differentiate the spile-reinforced shallow tunnel from the spile-reinforced deep tunnel is also formulated where the tunnel depth, soil type, geometry of the tunnel and reinforcing spiles, together with soil arching effects, are considered.

To examine the practical suitability of the proposed method of three-dimensional stability analysis, overall stability of the spile-reinforced shallow tunnel at facing is evaluated, and the predicted safety factors are compared with results from two-dimensional analyses.

Using the proposed method of three-dimensional limit equilibrium stability analysis of the spile-reinforced shallow tunnel in soft ground, effects of various design parameters such as tunnel depth, spile length and radial spile spacing are investigated. The parametric study may provide useful informations in designing spile-reinforced tunnel system.

The method of analysis proposed may be used to evaluate the overall stability or to determine the design parameters of the spile-reinforced shallow tunnel system or both. With slight modifications the analytical method of three-dimensional stability analysis proposed may also be extended for the analysis and design of steel pipe reinforced multi-step grouting technique frequently used as a supplementary reinforcing method in soft ground tunnel construction. However, the analytical findings need to be verified through systematic experimental studies. Continuous research is needed to deal with seepage forces, layered soil case, and spile-reinforced deep tunnel case.

Acknowledgements

Financial support for this study is provided by the Hong-Ik University(1996), and this support is gratefully acknowledged.

References

1. Bang, S.(1984) "Spiling Reinforcement System in Tunneling", *4th Australia-New Zealand Conference on Geomechanics,* Perth, Australia, pp.677-681.
2. Chen, R.H. and Chameau, J.L.(1982) "Three-Dimensional Limit Equilibrium Analysis of Slopes", *Geotechnique* 32, No. 1, pp.31-40.
3. Kim, H.T. and Kwon, Y.H.(1995) "Application of Soil Nailing Method to Tunnel Construction", *Proceedings of the KGS Spring '95 National Conference.*
4. Kim, H.T., Lee, W.J., and Sim, Y.J.(1996) "Study on Three Dimensional Stability Analysis of Spiling Reinforcement System", *Proceedings of the KGS Spring '96 National Conference.*
5. Korbin, G.E. and Brekke, T.L.(1976) "Model Study of Tunnel Reinforcement", *ASCE, Jour. of Geotech. Eng.,* Vol. 102. No. 9.
6. Korbin, G.E. and Brekke, T.L.(1978) "Field Study of Tunnel Prereinforcement", *ASCE, Jour. of Geotech. Eng.,* Vol. 104, No. 8.
7. Mostafa, A.R.(1982) "Stability Analysis of the Spiling Reinforcement System in Soft Ground Tunneling", *M.S. Thesis,* Univ. of Notre Dame, U.S.A.

(received on May, 17, 1997)